Formation of silver particles and periodic precipitate layers in silicate glass induced by thermally assisted hydrogen permeation

2001 J. Phys.: Condens. Matter 13 525

(http://iopscience.iop.org/0953-8984/13/3/312)

INSTITUTE OF PHYSICS PUBLISHING JOURNAL OF PHYSICS: CONDENSED MATTER

J. Phys.: Condens. Matter **13** (2001) 525–536 www.iop.org/Journals/cm PII: S0953-8984(01)15966-7

Formation of silver particles and periodic precipitate layers in silicate glass induced by thermally assisted hydrogen permeation

C Mohr[1], M Dubiel[1] and H Hofmeister[2]

[1] Martin Luther University of Halle-Wittenberg, Department of Physics, Friedemann-Bach-Platz 6, D-06108 Halle, Germany
[2] Max Planck Institute of Microstructure Physics, Weinberg 2, D-06120 Halle, Germany

Received 29 July 2000, in final form 9 October 2000

Abstract

Nanoscale silver particles embedded in sodium silicate glass were produced by Na/Ag ion exchange and subsequent thermal treatment in a hydrogen atmosphere. Their structure and spatial distribution were studied by conventional and high-resolution electron microscopy (HREM). Two different mechanisms of particle formation could be identified: (i) reduction of ionic silver by hydrogen and formation of mostly defective particles (twinned) within a near-surface region; and (ii) formation of single-crystalline particles in the interior of the glass resulting from reduction by means of polyvalent iron ions. Electron microscopy investigation revealed the completion of periodic layers of silver particles in near-surface regions with high silver concentration induced by thermally assisted hydrogen permeation. The self-organized periodic layer formation may be explained in terms of Ostwald's supersaturation theory, assuming interdiffusion of two mobile species. Analysis of lattice plane spacings from HREM images of silver particles revealed the typical size-dependent lattice contraction. The extent of this, however, was found to be different for particles formed by hydrogen permeation and those formed by interaction with polyvalent iron ions. These differences reflect different influences of the surrounding glass matrix, probably originating from the conditions of particle formation (thermal history).

1. Introduction

Nanoscale particles of transition metals like Ag, Au, and Cu embedded in silicate glass as the dielectric matrix have attracted much interest because of potential applications of such materials based on their non-linear optical properties [1, 2]. Many procedures like ion exchange and subsequent thermal treatment in different atmospheres or irradiation by highly energetic particles, ion implantation of metal ions, sol–gel synthesis, and multitarget magnetron sputtering onto SiO_2 have been used to incorporate small metal particles in glasses [3]. For some of these procedures, we have only very recently been able to show how the

0953-8984/01/030525+12$30.00

configuration and atomic structure of the particles are governed by the conditions of synthesis [4]. Accordingly, strong influences on the macroscopic properties of such nanoparticulate composites are expected. In glasses containing Ag or another metal in ionic form, thermal treatment under a hydrogen atmosphere is highly effective for inducing reduction and particle formation by aggregation of metal atoms [5–7]. Because of the excess availability of the highly reactive and mobile reducing agent, i.e. atomic hydrogen, a rather high density of metal particles is achieved in the hydrogen permeation region. According to the mechanism of reduction and particle formation under the hydrogen atmosphere, specific structures of the particles as well as the metal/glass interface are expected.

There has, however, been little knowledge disseminated about this procedure. The lattice parameter, as derived from x-ray diffraction, of silver particles formed in Vycor porous glass upon annealing at 450 °C in a hydrogen atmosphere was found to differ only slightly from the bulk value [8]. Layered precipitation of small copper particles in a near-surface region of soda-lime glass induced by hydrogen permeation was detected by means of scanning electron microscopy [9, 10]. Even if there is no constant period in the oscillations of such layered precipitate they are usually described as periodic. For Ag-doped glass, first hints as to periodic structures formed upon hydrogen treatment were obtained from optical spectroscopy studies [11]. From other investigations of silver particle formation in silicate glass upon hydrogen reduction, however, no such periodic precipitation was reported [6, 12, 13]. The formation of periodic structures, i.e. spatially separated precipitate regions of well defined width and spacing, induced by chemical reaction was first observed by Liesegang as self-organized concentric rings of precipitated silver dichromate [14]. Usually, such phenomena are explained by Ostwald's supersaturation theory of two mobile species diffusing into each other and forming insoluble precipitates in fluids as well as in solids.

The present paper introduces the structural characteristics of hydrogen-induced formation of silver particles and periodic precipitate layers in silicate glass as studied by conventional and high-resolution electron microscopy (HREM). In addition to outlining the spatial distribution of silver particles and the regularities of the precipitate layers, the dependence of the atomic structure of the particles on their location inside the glass is investigated. Two different formation mechanisms are established and discussed in terms of different reduction processes. From a lattice analysis, differences in the size-dependent lattice parameters of both types of particle are recognized which reflect certain changes in the interaction between the metal and the surrounding glass.

2. Experimental procedure

Soda-lime glasses containing 72.20% SiO_2, 14.20% Na_2O, 6.50% CaO, 4.42% MgO, 1.49% Al_2O_3, 0.71% K_2O, 0.13% Fe_2O_3, 0.39% SO_3 (in wt%) were immersed in a molten nitrate mixture of $NaNO_3$ and $AgNO_3$ at 330 °C, i.e. well below the glass transformation temperature of 535 °C, for 310 hours. By applying salt melt concentrations of 0.05 wt% and 5 wt% $AgNO_3$ in the Ag/Na ion exchange, two series of glass samples containing 0.8 and 11.0 mol% Ag_2O, respectively, were obtained. They are designated 'low Ag' and 'high Ag', respectively, throughout the following. We used thin glass slides of 160 μm thickness to achieve a nearly homogeneous distribution of silver ions inside the glass matrix as a result of ion exchange [15]. The reduction of ionic silver and the formation of crystalline precipitates in the nanometre size range was induced by five hours' subsequent annealing at 500 °C in hydrogen at atmospheric pressure. This treatment resulted in a non-homogeneous distribution of silver particles.

Cross-section preparation for the electron microscopy investigation of the glass samples was carried out by mechanical grinding, polishing, and careful ion-beam etching with Ar^+

ions, including liquid-nitrogen cooling followed by carbon coating to avoid charging effects. Special care was taken to avoid ion-beam thinning affecting the structures formed in the glass by ion exchange and subsequent annealing. Therefore, a low ion-beam current was applied and the specimens were cooled using liquid nitrogen. The shape and size of the particles as well as their spatial distribution were studied by conventional transmission electron microscopy (TEM) using a JEM 100C operating at 100 kV, whereas the high-resolution electron microscopy was done using a JEM 4000EX operating at 400 kV. The spacings of the (111) and (200) lattice planes of single-crystalline silver particles were determined by processing of digitized HREM images recorded under optimum conditions (near the Scherzer focus).

3. Results

3.1. TEM investigation

For the 'low-Ag' glass, five hours' exposure to hydrogen at 500 °C resulted in the formation of silver particles within a region of 3 μm thickness below the glass surface. Preceding studies by TEM and optical spectroscopy revealed, in both series of glass samples, no formation of silver particles upon ion exchange at 330 °C only. From TEM micrographs such as those shown in figure 1 it may be recognized that these particles have nearly spherical shape and are arranged at random in the glass matrix. The particle structure is characterized by the appearance of a great number of twin faults, i.e. single twins, parallel twin lamellae, and circular multiple

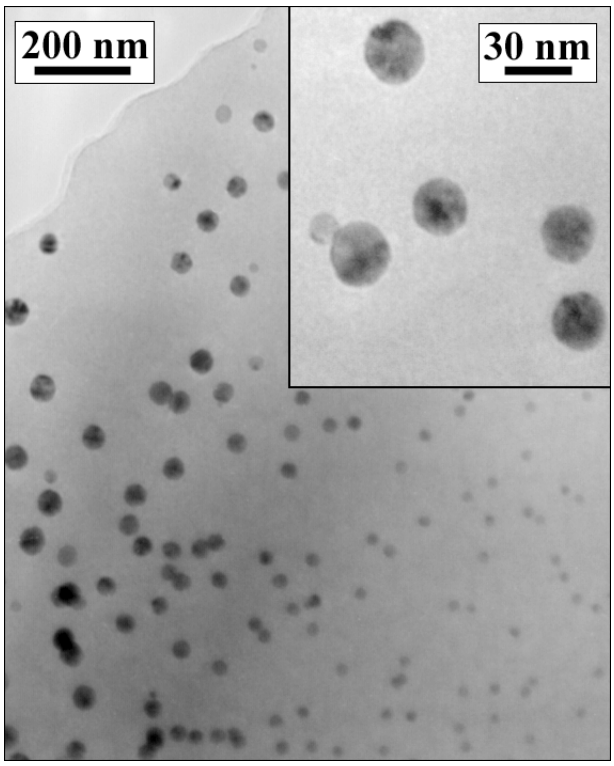

Figure 1. Particles in the 'low-Ag' glass at a penetration depth of 1.5 μm; the inset shows, at higher magnification, the non-homogeneous image contrast of some particles due to twin defects.

twins. There is a certain decrease in size and number density with increasing penetration depth. This continuous change ranging from ≈25 nm diameter very near the glass surface to ≈5 nm at about 2.5 μm penetration depth is graphically represented in figure 2. No periodicity or any modulation of the particle density was observed. Beyond 3 μm, no further Ag particles were found in this sample.

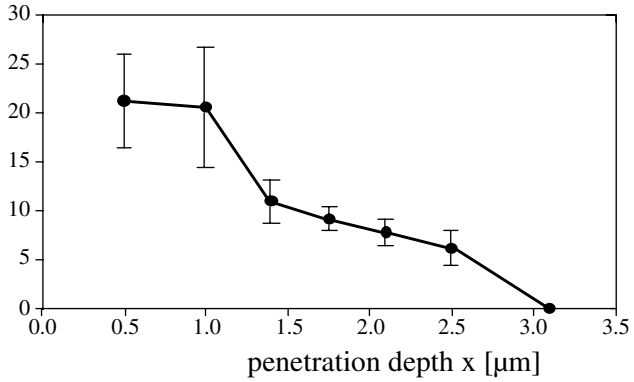

Figure 2. The dependence of the mean particle size of the 'low-Ag' sample on the penetration depth.

In the 'high-Ag' glass, five hours' exposure to hydrogen at 500 °C led to the formation of periodic layers of silver particles within a region of about 2 μm thickness below the glass surface. The electron micrographs of figures 3 and 4 demonstrate the layer constitution of the precipitates in this region and how the layer-like character results from densely arranged particles. The extension and 'periodicity' of these layers running parallel to the glass surface may be clearly recognized. These layers are designated by numbers in ascending order with increasing penetration depth. It can be seen that the nearer they are to the surface, the more the width and spacing of the layers decrease. Very near to the glass surface, some layers seem to overlap with each other, and it is not entirely clear how much of each one is included. Therefore, the first well separated single layer is numbered n and the other layers are counted according to this setting. As may be seen from figure 4, the spatial distribution of the particles is rather sharp with a steep transition at the layer boundaries. Within the periodic particle layers, the mean size and size distribution of the particles do not change very much. Figure 5 shows as an example the size distribution determined for particles of the layer $n+2$ that exhibit a log-normal shape with mean diameter $d_0 = 4.1$ nm and standard deviation $w = 0.32$ nm.

Below the $(n + 7)$th layer, no further layer-like particle distribution was observed, but around 5 μm penetration depth a second region of silver particles having a nearly homogeneous spatial distribution was found. This region ranges throughout the whole glass thickness until it meets the mirrored counterpart of the above-mentioned layer-like particle arrangement near the other surface of the 160 μm thick glass plate. The particle size variation throughout one half of the glass plate is shown in figure 6. Throughout the central 100 μm homogeneous glass region, a random arrangement of particles was found.

3.2. HREM investigation

HREM imaging of lattice plane fringes enabled us to recognize that in the region of hydrogen permeation, twin formation occurred for a large number of particles. To exclude the effects of varying twin configurations in the evaluation of size-dependent lattice parameters, particles

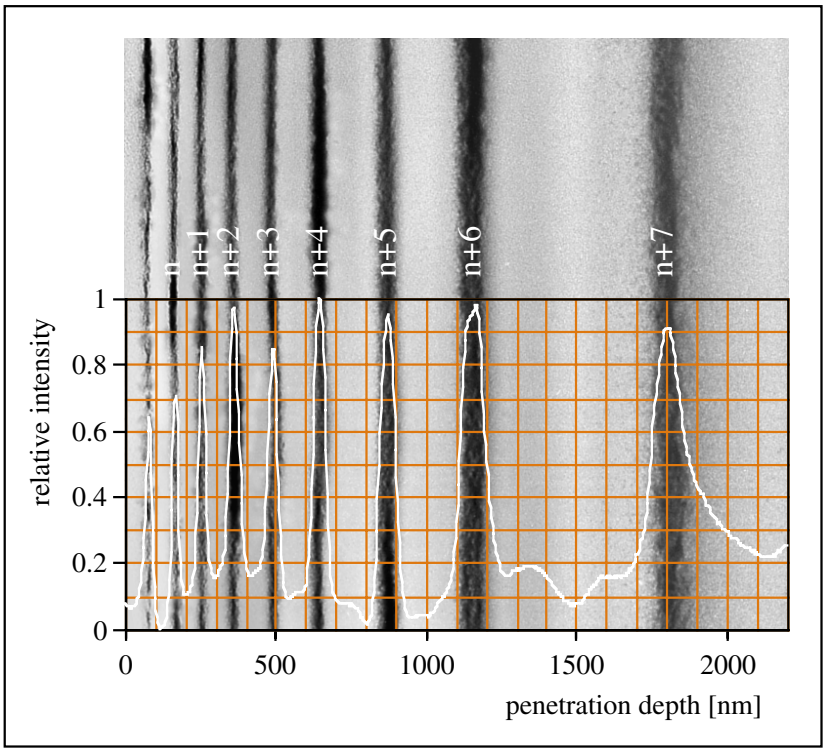

Figure 3. The near-surface region of the 'high-Ag' glass in a cross-sectional view together with a profile plot of the relative image intensity showing the arrangement and extension of the Ag precipitate layers.

containing twin faults were not considered. Instead, images of single-crystalline particles were chosen for the lattice analysis that was carried out in both real-space and Fourier-space (diffractogram) representations.

Owing to the surface curvature, small particles are usually in a state of compression [4, 16–20]. For the cubic lattice type, the resulting reduction of lattice spacing Δa is given by the Laplace-type equation

$$\Delta a = -\frac{2 f a \kappa}{3r} \tag{1}$$

where f is the surface stress, a is the bulk lattice parameter, κ is the compressibility, and r is the particle radius. For small particles embedded in a matrix, the surface stress is replaced by the interface stress f^*. Accordingly, size-dependent changes of the lattice spacing are determined by the value and sign of the interface stress. From the slope of the linear regression in the graphical representation of the lattice spacings versus particle size, as given in figure 7, the interface stress is evaluated according to equation (1). With the value for the compressibility of bulk silver $\kappa = 9.93 \times 10^{-12}$ m^2 N^{-1} we obtained $f^* = 1.0 \pm 0.6$ N m^{-1} for the 'low' glass, $f^* = 0.7 \pm 0.5$ N m^{-1} for the layer region, and $f^* = 2.0 \pm 0.7$ N m^{-1} for the central region of the 'high-Ag' sample. For comparison, figure 7 includes the size-dependent lattice parameters of both samples determined for particles from different regions.

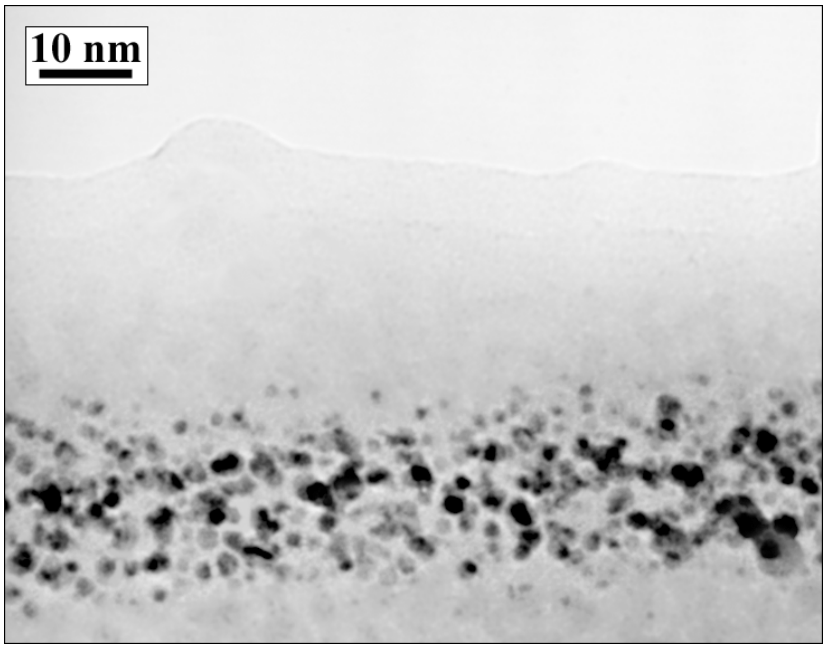

Figure 4. The distribution of Ag particles in one layer (n) of the 'high-Ag' glass.

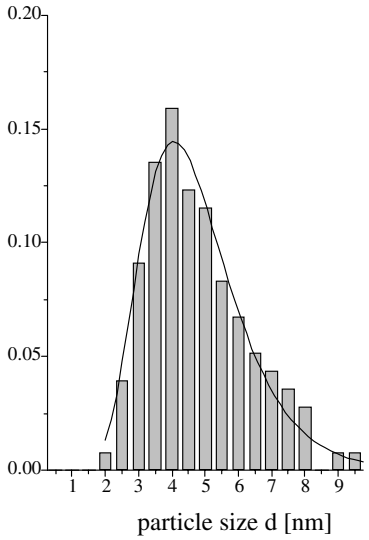

Figure 5. The relative particle size frequencies of the layer $n+2$ fitted by a log-normal distribution.

4. Discussion

4.1. Ag particle formation and periodic precipitation in the hydrogen permeation region

In the near-surface regions of both the 'low-Ag' and the 'high-Ag' samples, silver particles of similar structural characteristics are formed. Although their mean sizes differ considerably,

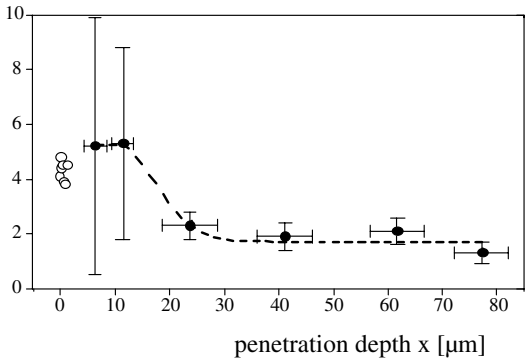

Figure 6. The dependence of the mean particle size of the 'high-Ag' sample on the penetration depth; small symbols indicate particles of the layer region and large symbols particles of the homogeneous region.

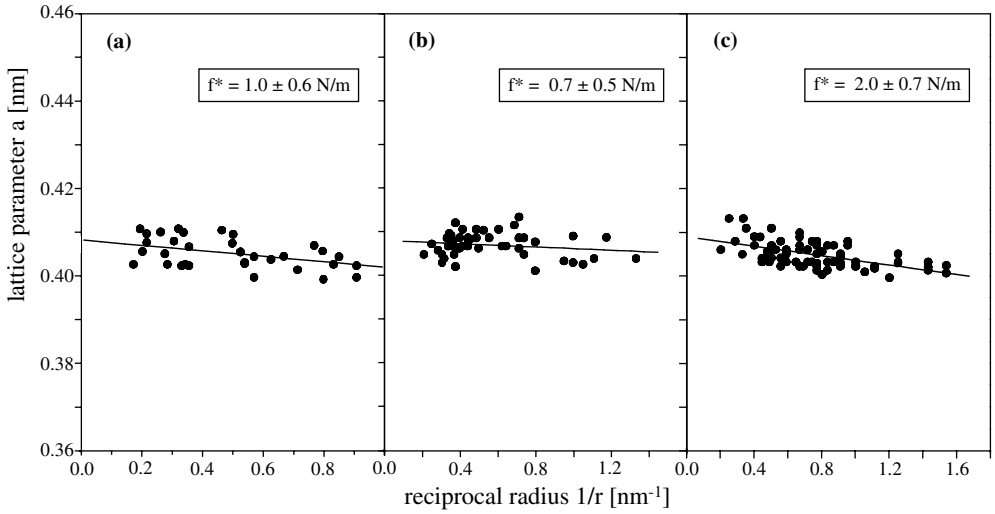

Figure 7. The lattice parameter determined from the (111) lattice plane fringes versus the inverse particle size in (a) the 'low' sample, (b) the layer region, and (c) the central region of the 'high' sample.

both exhibit plenty of twinned and multiply twinned structures. The basic mechanism of hydrogen-induced particle formation consists of two steps. It starts with silver ions which, due to ion exchange, replace sodium ions and are bonded to non-bridging oxygens. First, silver ions will be reduced by atomic hydrogen so as to form silver atoms and hydroxyl groups according to

$$\equiv\text{Si–O}^{-}\text{Ag}^{+} + (1/2)\text{H}_2 \rightarrow \equiv\text{Si–OH} + \text{Ag}^0. \tag{2}$$

These silver atoms are free to diffuse through the silicate network and form aggregates or clusters by successive addition of further silver atoms (see, e.g., [16–18]). The aggregation process results in Ag particles of nanometre size, observable by TEM. Because of the rather high hydrogen concentration, $c_{\text{H}} \gg c_{\text{Ag}}$, all silver ions present are expected to be thereby reduced. This assumption is justified by previous studies [6]. Consequently, a high concentration of Ag particles is formed which frequently contain planar lattice defects such as single- and

multiple-twin faults [21] owing to the rapid growth and particle interaction by coalescence. For the 'low' sample this may be recognized from figure 1. Despite the particle size decrease with increasing penetration depth, no distinct change of the lattice defect content was found. Obviously, the same mechanism of formation works throughout the whole region of hydrogen permeation.

Because there are considerably more silver ions incorporated in the 'high-Ag' sample, more complicated phenomena occur upon hydrogen-induced reduction. The layer-like spatial distribution of Ag particles near the glass surface is illustrated by figures 3 and 4. Liesegang's rings, or adequate layers in the two-dimensional case, develop sequentially upon the interdiffusion of two mobile species—here hydrogen and silver ions—always when the reaction product of both exceeds a certain supersaturation, thus giving rise to a spatially modulated density of precipitates. The formation of periodic layers of precipitates is described quantitatively for specific cases, e.g., for high enough initial concentrations of both species [22–25]. Then the layer formation starts at the interface between the reacting species sequentially in time, according to an asymptotic law [24]

$$x_n \sim (1 + \xi_*)^n x_0 \tag{3}$$

where x_n is the distance of the centre of the nth layer from the glass surface ($x = 0$) and ξ_*, x_0 are constants determining the spacing of consecutive layers. For the special case of one of the two mobile species being predominant in concentration, i.e. $A_0 \gg B_0$, the spatial separation of layers $\Delta x_n = x_{n+1} - x_n$ and the interval of their formation are predicted to satisfy the above asymptotic law with constant ratios of mutual spacings $\Delta x_{n+1}/\Delta x_n$ and consecutive distances x_{n+1}/x_n [22, 23, 25]. The time-dependent concentration of the reacting species as well as the positions of precipitated layers that develop at progressively greater distances from the initial interface may be calculated accordingly as functions of the experimental conditions, including the initial concentrations A_0 and B_0 and the corresponding diffusion constants D_A and D_B [22–25].

The parameters characteristic of the position and width of the silver particle layers are given in table 1. Because of uncertainties in accurately defining the position of the glass surface ($x = 0$) and the missing separation of the first $n - 1$ layers, some parameters, related to the onset of the periodic layer formation, deviate somewhat from the overall trend. Therefore, these values are given in brackets only. From table 1 and—even better—from figures 3 and 4 it can be seen that the spacing between two adjacent layers and the layer width increase with increasing distance from the glass surface which is the initial interface between the reacting species hydrogen and Ag^+. These results agree with the model predictions [22–25], giving strong indications of applicability of those models to the process studied here.

Table 1. Parameters characterizing the position, spacing, and width of the silver particle layers.

Layer	Layer position x_n (nm)	Layer spacing Δx_n (nm)	Layer width w (nm)	Distance ratio x_{n+1}/x_n	Mean particle size d (nm)
1 to $n-1$	78	—	(39)	—	3.7
n	168	(90)	36	(2.16)	3.5
$n+1$	255	87	55	1.52	4.1
$n+2$	360	105	66	1.41	3.6
$n+3$	488	128	72	1.36	3.8
$n+4$	646	158	76	1.32	3.4
$n+5$	873	228	83	1.35	3.9
$n+6$	1157	283	155	1.32	3.7
$n+7$	1802	645	252	1.55	4.0

Assuming a nearly homogeneous distribution of silver ions in the glass after Na/Ag ion exchange, particles may form upon silver-ion reduction by hydrogen, within the corresponding permeation region, and subsequent aggregation to stable Ag precipitates. With hydrogen being the predominant species in this region, i.e., $c_H \gg c_{Ag}$, all silver species are assumed to be neutral atoms which will be incorporated almost completely in growing Ag particles when a certain supersaturation is attained. By taking into consideration that the rate of hydrogen diffusion is much less than the rate of silver-ion reduction, it may be understood that in a layer of certain depth below the glass surface and of certain thickness, all silver ions will be reduced and consumed in particle formation. A new layer of particles will form only at somewhat larger depth after enough silver reaches that depth. In this way, periodic layers of particles are formed within the region of hydrogen permeation if a sufficient amount of silver is available.

From equation (3) the spacing parameter ξ_* can be calculated using the data on the observed layers; this yields an average value of $\xi_* \simeq 0.40 \pm 0.15$. With the Prager–Zeldovitch solution [22, 23] such a value is found for $D_{Ag} > D_H$ which is common for sodium silicate glass. For example, Miotello *et al* [12] calculated the corresponding diffusion parameters from hydrogen permeation in Ag/Na ion-exchanged glasses at 180 °C as $D_{Ag} = 1.2 \times 10^{-14}$ cm^2 s^{-1} and $D_H = 6 \times 10^{-15}$ cm^2 s^{-1}, in agreement with the above assumption. Similar data are reported by Frischat [25]. Here, the penetration depth of hydrogen estimated from the surface region containing highly agglomerated silver particles is 1.5 μm (see figure 4). Consequently, the formation of periodic precipitates in Ag/Na ion-exchanged glass can be described by Ostwald's supersaturation model assuming two mobile species which react to induce particle formation and growth. The data shown in table 1 indicate that the mean size of Ag particles throughout the various layers is approximately constant. That means that an increase of the particle size with increasing distance from the surface like that observed for reduction by hydrogen in copper-containing soda-lime silicate glass [10] was clearly not found.

In the 'low-Ag' sample the formation of silver particles occurred within a near-surface region of about 3 μm thickness, whereas the remaining glass region remains free of any particles. Obviously, under the conditions applied, the particle formation is restricted to the region of hydrogen permeation, and beyond that region no other reducing agents such as polyvalent ions have any effect. This implies also the absence, or the removal, of silver ions from the deeper region, which may be caused by processes quite similar to those occurring in the near-surface region of the 'high-Ag' sample which occur here—however, under changed conditions. The main difference is the rather low content of silver (0.8 mol% Ag_2O as compared to 11 mol%) from which the spacing parameter ξ_* is estimated according to the model computation of the reaction processes [22, 25] to be exceedingly large ($\gg$10) as compared to that of the 'high-Ag' sample. Additionally, extended layer formation periods, enlarged layer spacings, and increased layer widths, exceeding by far the experimental limitations, must be expected. Therefore, no layer-like arrangement of Ag particles was achieved in the 'low-Ag' sample. Generally, one needs an appropriate concentration of silver ions, duration of the heat treatment, and resolution of the detection method in order to identify periodic precipitates upon hydrogen-induced particle formation in silver-doped glasses. The corresponding investigations of such glasses have failed up to now in this respect [6, 12, 13].

4.2. Ag particle formation without hydrogen permeation

The silver particles found in regions deeper than about 5 μm in the 'high-Ag' glass exhibit an internal structure different from that of particles in the near-surface hydrogen-permeated regions of both samples. Most of them are single-crystalline particles without any twin planes. They have sizes of about 2 nm within an extended central region, whereas towards the glass

surface an increase to 5 nm is observed. The mechanism of particle formation in these regions without hydrogen permeation is expected to be based on Fe^{2+} ions as reducing agents. As supported by optical spectroscopy, transmission electron microscopy, and x-ray absorption spectroscopy studies [4, 26, 27], the following reaction is most probably active in soda-lime glass:

$$Ag^{+} + Fe^{2+} \rightarrow Ag^{0} + Fe^{3+}. \tag{4}$$

The possibility of the extraction of electrons intrinsic to the glass network as proposed by Araujo [28] can be excluded because of the low proportion of non-bridging oxygens and the presence of polyvalent iron ions. Due to their small concentration (0.05 mol% Fe_2O_3), however, most of the silver species within the central glass region remain in the ionic state. They have a high mobility (see the diffusion parameter mentioned above [12]) in contrast to clusters or aggregates of neutral silver atoms. Because of the hydrogen-induced precipitation in near-surface regions of the glass, as well as some thermally assisted evaporation of silver at the glass surface, a certain proportion of the silver ions originally situated within the central region of the sample are expected to move outwards. That should lead to a depletion of the silver species, at first, at the boundary of the central region and the hydrogen-containing region. This depletion will strengthen during hydrogen-induced formation of Ag precipitates. As a consequence of this depletion, the Ag nucleation rate in this region decreases, yielding a reduced number of particles with increasing size of up to 5 nm. This effect is comparable to the particle size increase at the edge of the silver-containing surface layer upon ion exchange and subsequent annealing without hydrogen in glass samples whose thickness exceeds by far the silver-ion penetration depth [26].

4.3. Ag particle size and interface effects

The rather different appearance of particles in samples of different Ag concentrations, on the one hand, and in regions with different particle formation mechanisms of the 'high-Ag' sample on the other hand, suggested a study of the influence of these conditions on the glass/metal interaction across the particle–matrix interface. Changes of this interaction are sensitively reflected by the lattice parameter of the particles, the size dependence of which determines the interface stress f^*. The interface stress, in turn, is a measure of the strength of interaction across the particle/matrix interface. In fact, as mentioned above, this interface stress varies characteristically according to the conditions applied. For particles formed in near-surface hydrogen-permeation regions of the 'low-Ag' and the 'high-Ag' sample, interface stress values of 1.0 and 0.7 N m^{-1}, respectively, were obtained, whereas for silver particles in the central region of the 'high-Ag' sample, 2 N m^{-1} was obtained. These variations point to the influence of the specific mode of silver-ion reduction and mechanism of particle formation.

In a previous study we obtained for silver particles, formed in ion-exchanged glass upon annealing at 635 °C, an interface stress of 4.5 N m^{-1} [4]. Comparison of this value to the above-mentioned value 2 N m^{-1} from the present study obtained for particles from hydrogen-free glass regions indicates that the different thermal histories of these samples (400 °C compared with 330 °C for ion exchange and 635 °C compared with 500 °C for annealing) sensitively influence the particle/matrix interaction. In contrast to this, distinctly smaller interface stress values are found for particles in the hydrogen-permeated region of both the 'low-Ag' and the 'high-Ag' glass samples. Since reduction of silver ions by hydrogen is accompanied by extensive incorporation of hydroxyl groups into the glass matrix, the above findings point to the importance of the glass network structure for the effects studied here.

5. Conclusions

Thermally assisted permeation of hydrogen into Ag/Na ion-exchanged glass rather effectively causes reduction of the Ag ions and precipitation of metallic Ag particles, whose defect configuration is due to the rapid growth from the supersaturated solid solution. The spatial distribution of the particles formed does not exhibit indications of periodicity or density modulation unless the silver doping is so high that, sequentially in time and penetration depth, a sufficient supersaturation of atomic silver is attained that a system of layered precipitates is achieved. The formation and structural peculiarities of these silver particle layers may be explained in terms of Ostwald's supersaturation theory assuming hydrogen and silver ions as mobile species. This process of self-organization takes place on a scale of less than 2 μm; thus it needs electron microscopy to disclose details such as the layer position and width.

In the interior of the highly doped glass sample another particle formation mechanism, based on Ag^+ reduction by means of Fe^{2+} ions, was active. The particles formed thereby exhibit no indications of periodic arrangement—but rather a random arrangement. In contrast to the mostly defective particles in the near-surface region for the two samples, the internal reduction leads to mostly single-crystalline particles. Since these different particle formation mechanisms are accompanied by various modifications of the glass network structure, different interface effects reflected by corresponding interface stress values are observed. Efforts are in progress now to relate these differences to certain processes and structures relating to the particle/matrix interface.

Acknowledgment

This work was supported by the Deutsche Forschungsgemeinschaft (SFB 418).

References

[1] Hacke F, Ricard D and Flytzanis C 1986 *J. Opt. Soc. Am.* B **3** 1647
[2] Maruyama O, Senda Y and Omi S 1999 *J. Non-Cryst. Solids* **259** 100
[3] Gonella F and Mazzoldi P 2000 *Handbook of Nanostructured Materials and Nanotechnology* vol IV, ed H S Nalwa (San Diego, CA: Academic) p 81
[4] Dubiel M, Hofmeister H and Schurig E 1998 *Recent Res. Dev. Appl. Phys.* **1** 69
[5] Barton J L and Morain M 1970 *J. Non-Cryst. Solids* **3** 115
[6] De Marchi G, Caccavale F, Gonella F, Mattei G, Mazzoldi P, Battaglin G and Quaranta A 1996 *Appl. Phys.* A **63** 403
[7] Roy B, Jain H, Roy S and Chakravorty D 1997 *J. Non-Cryst. Solids* **222** 102
[8] Yanase A, Komiyama H and Tanaka K 1990 *Surf. Sci. Lett.* **226** L65
[9] Estournes C, Cornu N and Guille J L 1994 *J. Non-Cryst. Solids* **170** 287
[10] Estournes C, Cornu N, Guille J L, Epicier T, Wang L C and Lehuede P 1996 *Phys. Chem. Glasses* **37** 177
[11] Berg G 1999 *Martin-Luther-University Halle-Wittenberg Internal Report* B5 of SFB 418 (Halle) p 253
[12] Miotello A, De Marchi G, Mattei G and Mazzoldi P 1998 *Appl. Phys.* A **67** 527
[13] Borsella E, Cattaruzza E, De Marchi G, Gonella F, Mattei G, Mazzoldi P, Quaranta A, Battaglin G and Polloni R 1999 *J. Non-Cryst. Solids* **245** 122
[14] Liesegang R E 1896 *Naturwiss. Wochenschr.* **11** 353
Liesegang R E 1896 *Photogr. Arch.* **21** 221
Liesegang R E 1896 *Photogr. Arch.* **37** 321
[15] Dubiel M, Brunsch S and Tröger L 2000 *J. Phys.: Condens. Matter* **12** 4775
[16] Solliard C and Flueli M 1985 *Surf. Sci.* **156** 487
[17] Kreibig U 1976 *Appl. Phys.* **10** 255
[18] Henglein A, Mulvaney P and Linnert T 1991 *Faraday Discuss.* **92** 31
[19] Belharouak I, Parent C, Tanguy B, Le Flem G and Couzi M 1999 *J. Non-Cryst. Solids* **244** 238
[20] Vermaak J S, Mays C W and Kuhlmann-Wilsdorf D 1968 *Surf. Sci.* **12** 128

[21] Hofmeister H 1998 *Cryst. Res. Technol.* **33** 3
[22] Prager S 1956 *J. Chem. Phys.* **25** 279
[23] Zeldovitch Ya B, Barenblatt G I and Salganik R L 1962 *Sov. Phys.–Dokl.* **6** 869
[24] Kai S, Müller S and Ross J 1982 *J. Chem. Phys.* **76** 1392
[25] Frischat G H 1975 *Ionic Diffusion in Oxide Glasses* ed Y Adda, A D Le Claire, L M Slifkin and F H Wöhlbier (Zurich: Trans Tech) p 128
[26] Berg K-J, Berger A and Hofmeister H 1991 *Z. Phys.* D **20** 309
[27] Dubiel M, Brunsch S, Brenn U and Schwieger W 1998 *Proc. 18th Int. Glass Congr. (San Francisco, CA, 1998)* pp PO2–192
[28] Araujo R 1992 *Appl. Opt.* **31** 5221